Comprehensive Studies on Mechanical Stress Analysis of Functionally Graded Plates

Kyung-Su Na, and Ji-Hwan Kim

***Abstract*—**Stress analysis of functionally graded composite plates composed of ceramic, functionally graded material and metal layers is investigated using 3-D finite element method. In FGM layer, material properties are assumed to be varied continuously in the thickness direction according to a simple power law distribution in terms of the volume fraction of a ceramic and metal. The 3-D finite element model is adopted by using an 18-node solid element to analyze more accurately the variation of material properties in the thickness direction. Numerical results are compared for three types of materials. In the analysis, the tensile and the compressive stresses are summarized for various FGM thickness ratios, volume fraction distributions, geometric parameters and mechanical loads.

***Keywords*—**Functionally graded materials, Stress analysis, 3-D finite element method

I. Introduction

FUNCTIONALLY graded materials (FGMs) are nonhomogeneous materials in which material properties are changed gradually from one surface to the other. Typically these materials are composed of engineering ceramics and light metals. A ceramic is useful in high compressive strength and temperature applications, however suffers from low fracture toughness. On the contrary, a metal exhibits better tensile strength and thermal shock resistance but cannot withstand exposure to high temperatures. From the mixture of these materials, FGMs can withstand high-temperature environments while maintain their structural integrity. Thus, FGMs have been researched and developed in many engineering filed, such as the future space-planes, nuclear plants and fusion reactors, etc.

Reddy and Chin [1] studied the dynamic thermoelastic response of cylinders and plates. The three-dimensional heat conduction and the thermoelastic equations were solved. Na and Kim [2] investigated the three-dimensional thermomechanical buckling analysis of plates by using finite element method. In this, an 18-node solid element and the assumed strain mixed formulation were applied. Najafizadeh and Eslami [3] discussed the thermal buckling of a circular plate under three types of thermal loads. The nonlinear equilibrium and linear stability equations were derived using variational formulations. Nakamura et al. [4] introduced a new measurement procedure based on inverse analysis and instrumented micro indentation. The inverse analysis was utilized to extract information from indented load-displacement data beyond usual parameters such as elastic modulus. Yang and Shen [5] analyzed the nonlinear bending of shear deformable plates subjected to thermo-mechanical loads under various boundary conditions. Ma and Wang [6] investigated the axisymmetric large deflection bending and thermal post-buckling of a circular plate under mechanical, thermal and combined thermal-mechanical loadings. Vel and Batra [7] presented an analytical solution for three-dimensional thermomechanical deformations of a simply supported rectangular plate subjected to time-dependent loads on its top and/or bottom surfaces. Qian et al. [8] analyzed the static deformations, and free and forced vibrations of a thick rectangular plate by using a higher-order shear and normal deformable plate theory. Jin and Batra [9] studied the effects of loading conditions, specimen size and metal particle size on the crack growth resistance curve (R-curve) and residual strength of a model based on the crack-bridging concept.. Tanaka et al. [10] formulated a method of macroscopic material tailoring in order to reduce globally the thermal stresses induced in the FGMs. FGM. Li et al. [11] presented the mode I stress intensity factors for FGM solid cylinders with an embedded penny-shaped crack or an external circumferential crack. Oota et al. [12] applied a genetic algorithm to an optimization problem of minimizing the thermal stress distribution for a plate of step-formed FGMs. Cho and Choi [13] explored the suitability of the yield-stress-calibrated objective function for maximizing the yield strength of heat-resisting FGMs.

In this work, the stress analysis considering tensile and compressive stress ratios is analyzed for FGM composite plates using 3-D finite element method. An 18-node solid element is selected for more accurate modeling of material properties in the thickness direction. In FGM layer, material properties are assumed to be varied continuously in the thickness direction according to a simple power law distribution in terms of the volume fraction of a ceramic and metal. In addition, the effective material properties are obtained according to the linear rule of mixtures. Furthermore, the tensile and the compressive stresses according to the FGM thickness ratio, volume fraction distribution, geometric parameter and mechanical load are analyzed, in detail.

II. Modeling of FGM Composite Plates

A FGM composite plate is made up of ceramic, FGM, and metal layers, of length a, width b, and thickness h. Further, h_c, h_m and h_f indicate the thicknesses of ceramic, metal and FGM layers, respectively. The thickness ratios of ceramic, metal, and FGM layers are denoted by r_c, r_m and r_f, respectively, and they are expressed as

Kyung-Su Na was with School of Mechanical and Aerospace Engineering, Seoul National University, Seoul, Korea and currently, is with Satellite group, Korea Institute of Aerospace Technology, Korean Air, Yusung-Gu, Daejeon 461-1, Korea (e-mail: carcass11@hanmail.net).

Ji-Hwan Kim is with School of Mechanical and Aerospace Engineering, Seoul National University, Seoul, Korea (e-mail: jwhkim@snu.ac.kr).

$$r_f = \frac{h_f}{h}, \quad r_c = \frac{h_c}{h} = r_m = \frac{h_m}{h} = \frac{1}{2}\left(1 - r_f\right) \tag{1}$$

The volume fraction of metal V_m is given by applying a simple power law distribution. Also, the volume fraction of ceramic V_c can be obtained as

$$V_c(z) = 1 - V_m(z) \tag{2}$$

According to the linear rule of mixtures, the effective material properties P_{eff} can be obtained as in [1].

$$P_{eff}(z) = P_m V_m(z) + P_c V_c(z) \tag{3}$$

where P_m and P_c represent the material properties of the metal and ceramic, respectively.

III. 3-D Finite Element Method

Considering a three-dimensional solid body in equilibrium,

$$\int \delta \mathbf{E}^T \mathbf{S} dV - \delta \mathrm{W} = 0 \tag{4}$$

where $\delta\mathbf{E}$, $\mathbf{S}$, δW and V indicate the virtual strain vector expressed in terms of the displacement vector $\mathbf{u}$, the 2nd Piola-Kirchhoff stress vector, the external virtual work and the volume of the undeformed configuration, respectively. The stress vector $\mathbf{u}$ is related to the strain vector $\mathbf{E}$ through the following equations.

$$\mathbf{S} = \mathbf{C}(\mathbf{E} - \mathbf{E}^{\mathbf{th}}) \tag{5}$$

where C is the 6×6 elastic matrix of material stiffnesses, defined in the local coordinate system. Additionally, the thermally-induced strain vector $\mathbf{E}$ th is defined in the thermal environment.

Using 3D finite element discretization, and assembling over all elements, then

$$\delta \mathbf{q}^T (\mathbf{K}\mathbf{q} - \mathbf{Q}) = 0 \tag{6}$$

IV. Stress Analysis under Mechanical Load

The stress analysis of FGM composite plates under mechanical load is studied for clamped cases. In here, Si_3N_4/SUS304, Al_2O_3/Ni and ZrO_2/Ti-6Al-4V are chosen to be the constituent materials. Using the nondimensionalization, the tensile stress and the compressive stress ratios of the structure under sinusoidal load are investigated for various FGM thickness ratios, volume fraction distributions, geometric parameters and mechanical loads. Furthermore, all data are given for a/h =50, $\overline{q}$ =5.

Additionally, the thickness ratio of the metal and the ceramic layers are assumed to be same as

$$r_m = r_c = (1 - r_f)/2 \tag{7}$$

Temperature dependent material properties are listed in [12]. Additionally, material properties at room temperature for 300K are used. as a reference temperature T_{ref}.

To evaluate the stress distribution, the tensile and the compressive stresses are analyzed. Sinusoidal load q_3 is given by the expression

$$q_3 = -\overline{q}_3 \sin \pi\overline{x} \sin \pi\overline{y} \tag{8}$$

where $\overline{q}_3 = \overline{q}\ E_m \left(\frac{h}{a}\right)^4$

in which $\overline{q}_3$ represents the intensity of the load at the center of the plate and E_m indicates Young's modulus of metal. The tensile strength σ_{Bt} and the compressive strength σ_{Bc} for ceramics and metals are appeared in [12]. In the data, the compressive strength of a ceramic is larger than that of a metal, while, the tensile strength of a ceramic is smaller than that of a metal. Based on the linear rule of mixtures, the tensile and the compressive strengths of the plates at each point are assumed as

$$\begin{aligned} \sigma_{Bt}(\overline{z}) &= \sigma_{Btm} V_m(\overline{z}) + \sigma_{Btc} V_c(\overline{z}) \\ \sigma_{Bc}(\overline{z}) &= \sigma_{Bcm} V_m(\overline{z}) + \sigma_{Bcc} V_c(\overline{z}) \end{aligned} \tag{9}$$

Fig. 1 depicts the tensile and compressive strengths of Si_3N_4/SUS304 FGM composite plates along the thickness direction.

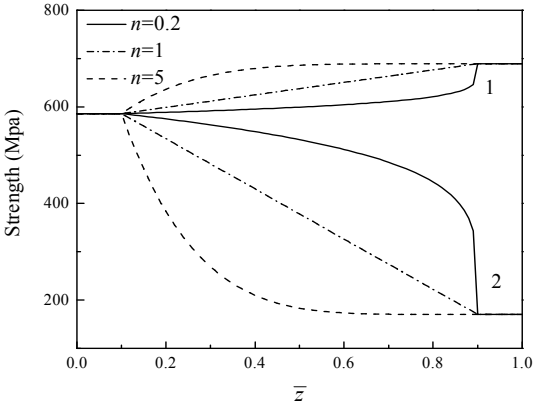

Fig. 1 Tensile and compressive strengths of Si_3N_4/SUS304 FGM composite plates along the thickness direction (r_f =0.8).

In the figure, 1 and 2 indicate σ_{Bc} and σ_{Bt}, respectively. When $\overline{z}$ is increased, the compressive strength increases, however, the tensile strength decreases in FGM layer. Therefore, to evaluate the stress according to the strength, the

stress ratio σ^* is introduced by using the tensile stress ratio $\bar{\sigma}_t$ and the compressive stress ratio $\bar{\sigma}_c$, as

$$\sigma^* = \begin{cases} \bar{\sigma}_t = \sigma_{xx} / \sigma_{Bt} & \sigma_{xx} \geq 0 \\ \bar{\sigma}_c = \sigma_{xx} / \sigma_{Bc} & \sigma_{xx} \leq 0 \end{cases} \quad (10)$$

In this equation, to avoid failure, the condition $|\sigma^*|$ <1 should be fulfilled and when $|\sigma^*|$ becomes small, the structure achieves better stress reduction.

A. $Si_3N_4 / SUS304$

The maximum tensile stress $(\bar{\sigma}_t)_{\max}$ according to FGM thickness ratio and volume fraction index is shown in Table I.

TABLE I
MAXIMUM TENSILE STRESS $(\bar{\sigma}_t)_{\max}$ ACCORDING AS FGM THICKNESS RATIO AND VOLUME FRACTION INDEX

n	r_f			
	0	0.4	0.6	1
0.2	0.4563	0.4618	0.4736	0.2158
0.5	0.4563	0.4591	0.4649	0.3471
1	0.4563	0.4574	0.4590	0.4392
2	0.4563	0.4566	0.4557	0.4480
5	0.4563	0.4563	0.4535	0.4365

In FGM composite plates, as the volume fraction index is increased, the tensile stress decreases. However, in fully FGM plates for r_f equal to1, when $n \leq 2$, the tensile stress increases, while in the other region, it decreases as n is increased. When $n \geq 2$,the tensile stress decreases as the FGM thickness ratio r_f is increased. In all cases of n, the tensile stresses have the smallest values when r_f is 1. In addition, the tensile stress has the smallest when r_f is 1 and n is the smallest, but it is largest when r_f is 0.6 and n is the smallest. It is observed that the effect of n is greatest when r_f is 1.

Table II illustrates the maximum compressive stress $|\bar{\sigma}_c|_{\max}$ with respect to FGM thickness ratio and volume fraction index. When the volume fraction index n is increased, the compressive stress decreases. This is because the contained quantity of ceramic increases as the volume fraction index is increased.When $n \geq 1$, the compressive stress decreases as the FGM thickness ratio r_f is increased.The compressive stress has the smallest value when r_f is 1 and n is the largest, while it has the largest value when r_f is 1 and n is the smallest. This phenomenon is very similar to that of the displacement.

TABLE II
MAXIMUM COMPRESSIVE STRESS $|\bar{\sigma}_c|_{\max}$ WITH RESPECT TO FGM THICKNESS RATIO AND VOLUME FRACTION INDEX

n	r_f			
	0	0.4	0.6	1
0.2	0.1093	0.1093	0.1094	0.1137
0.5	0.1093	0.1090	0.1085	0.1090
1	0.1093	0.1085	0.1075	0.1050
2	0.1093	0.1078	0.1060	0.1011
5	0.1093	0.1066	0.1035	0.0961

From Tables I and II, in overall cases, the tensile stress ratios have larger values than the compressive stress ratios. Thus, the tensile stress is the most important factor for evaluation of maximum stress ratio for the FGM composite plates under mechanical load. Through-the-thickness distributions of the stress ratio σ^* with various volume fraction indexes are depicted in Fig. 2 and 3.

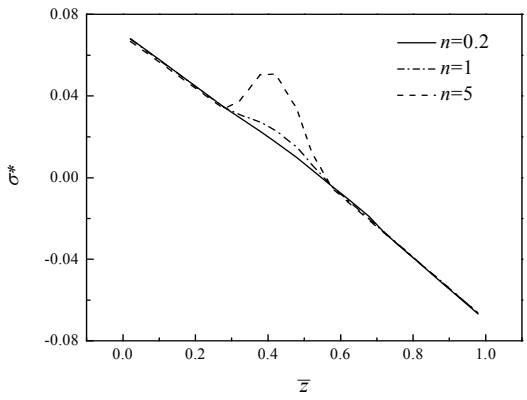

Fig. 2 Through-the-thickness distribution of the stress ratio σ^* according to volume fraction index (r_f = 0.4).

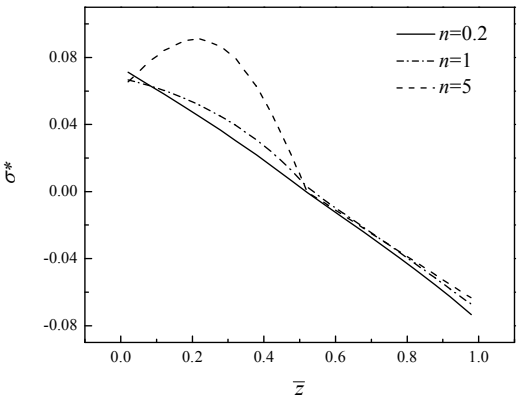

Fig. 3 Through-the-thickness distribution of the stress ratio σ^* with respect to volume fraction index (r_f = 1).

The stress concentrations are observed in FGM layer and they are considerable at the metal-FGM layer interface for relatively large n. The concentrations are relaxed when volume fraction index is decreased and become smooth as the FGM thickness ratio is increased. The stress ratio increases when the volume fraction index is increased in the region $\bar{z} \leq 0.5$. In the case of n =0.2, the smoothest stress distribution is observed.

As a result, the absolute value of stress ratio $|\sigma^*|$ has the smallest value and the stress distribution shows the smoothest response for the smallest n and for the fully FGM plates.

B. Al_2O_3 / Ni

Table III illustrates the maximum tensile stress $(\bar{\sigma}_t)_{\max}$ of Al2O3/Ni FGM composite plates with variations of FGM thickness ratio and volume fraction index.

TABLE III
MAXIMUM TENSILE STRESS $(\bar{\sigma}_t)_{\max}$ OF Al_2O_3/Ni FGM COMPOSITE PLATES ACCORDING TO FGM THICKNESS RATIO AND VOLUME FRACTION INDEX

n	r_f			
	0	0.4	0.6	1
0.2	0.3027	0.3064	0.3146	0.2741
0.5	0.3027	0.3046	0.3086	0.3018
1	0.3027	0.3035	0.3046	0.3050
2	0.3027	0.3030	0.3024	0.2973
5	0.3027	0.3028	0.3009	0.2890

In FGM composite plates, as the volume fraction index is increased, the tensile stress ratio decreases. However, in fully FGM plates, when $n \leq 1$, the tensile stress increases, while in the other region, it decreases as n is increased. When $n \geq 2$, the tensile stress decreases as the FGM thickness ratio r_f is increased. The tensile stress ratio has the smallest value when r_f is 1 and n is the smallest, on the contrary, it is largest when r_f is 0.6 and n is the smallest. The effect of n is greatest when r_f is 1.

TABLE IV
MAXIMUM COMPRESSIVE STRESS $|\bar{\sigma}_c|_{\max}$ OF Al_2O_3/Ni FGM COMPOSITE PLATES WITH RESPECT TO FGM THICKNESS RATIO AND VOLUME FRACTION INDEX

n	r_f			
	0	0.4	0.6	1
0.2	0.1987	0.1987	0.1989	0.2001
0.5	0.1987	0.1980	0.1972	0.1822
1	0.1987	0.1971	0.1951	0.1627
2	0.1987	0.1957	0.1922	0.1369
5	0.1987	0.1935	0.1876	0.0961

The maximum compressive stress $|\bar{\sigma}_c|_{\max}$ with respect to FGM thickness ratio and volume fraction index is presented in Table IV. The compressive stress ratio decreases as the volume fraction index n is increased. When $n \geq 0.5$, the compressive stress decreases as the FGM thickness ratio r_f is increased. The compressive stress has the smallest value when r_f is 1 and n is the largest, while it has the largest value when r_f is 1 and n is the smallest. In Tables III and IV, it is observed that the tensile stress ratios have larger values than the compressive stress ratios.

Fig. 4 depicts through-the-thickness distribution of the stress ratio σ^* for Al_2O_3/Ni FGM composite plates when the FGM thickness ratio is 0.4 for (a) and 1 for (b).

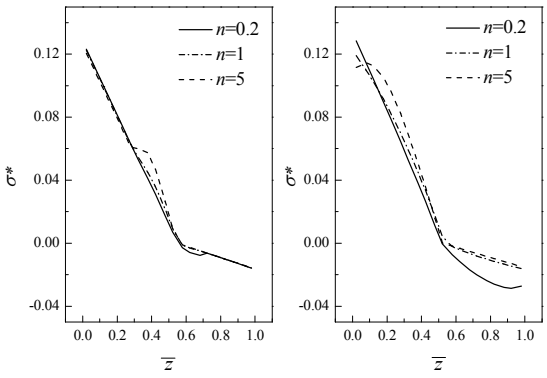

(a) r_f =0.4 (b) r_f =1

Fig. 4 Through-the-thickness distribution of the stress ratio σ^* with variation of volume fraction index

In Fig.4, when n is 0.2, small stress concentration is observed at the FGM-ceramic interface ($\bar{z}$ =0.7). However, when n is 5, larger stress concentration is shown at the metal-FGM layer interface ($\bar{z}$ =0.3). In Fig. 4 (b), it is shown that the stress concentration is relaxed, while the compressive stress increases in the region $\bar{z} \geq 0.5$, especially when n is 0.2. In overall view of the results, the smoothest stress distribution is observed in the case of n =0.2. As a consequence, for the smallest n and for the fully FGM plates, the absolute value of stress ratio $|\sigma^*|$ has the smallest value and the stress distribution shows the smoothest response.

C. ZrO_2 / Ti - 6Al - 4V

The maximum tensile stress $(\bar{\sigma}_t)_{\max}$ of ZrO_2/Ti-6Al-4V FGM composite plates according to FGM thickness ratio and volume fraction index is shown in Table V. In FGM composite plates, as the volume fraction index is increased, the tensile stress ratio decreases with small amount. On the contrary, in fully FGM plates it shows a different response. When $n \leq 2$, the tensile stress increases, while in the other region, it decreases as n is increased.

When $n \geq 2$, the tensile stress decreases as the FGM thickness ratio r_f is increased.In all cases of n, the tensile

stresses have the smallest values when r_f is 1. In addition, the tensile stress has the smallest when r_f is 1 and n is the smallest, however it is largest when r_f is 0.6 and n is the smallest. Furthermore, the effect of n is greatest when r_f is 1.

TABLE V
MAXIMUM TENSILE STRESS $(\bar{\sigma}_t)_{\max}$ OF ZrO_2/Ti-6Al-4V FGM COMPOSITE PLATES ACCORDING TO FGM THICKNESS RATIO AND VOLUME FRACTION INDEX

n	r_f			
	0	0.4	0.6	1
0.2	0.2536	0.2549	0.2573	0.0685
0.5	0.2536	0.2543	0.2556	0.1387
1	0.2536	0.2540	0.2544	0.2273
2	0.2536	0.2538	0.2538	0.2524
5	0.2536	0.2538	0.2535	0.2511

Table VI illustrates the maximum compressive stress $|\bar{\sigma}_c|_{\max}$ with respect to FGM thickness ratio and volume fraction index. The compressive stress ratio decreases, as the volume fraction index n is increased. When $n \geq 1$, the compressive stress decreases as the FGM thickness ratio is increased. The compressive stress has the smallest value when r_f is 1 and n is the largest, while it has the largest value when r_f is 1 and n is the smallest. From Tables V and VI, in overall cases, the tensile stress ratios have larger values than the compressive stress ratios. This shows that the tensile stress is more important factor than the compressive stress for evaluation of maximum stress ratio for the FGM composite plates under mechanical load.

TABLE VI
MAXIMUM COMPRESSIVE STRESS $|\bar{\sigma}_c|_{\max}$ $(\times 10^{-1})$ OF ZrO_2/Ti-6Al-4V FGM COMPOSITE PLATES WITH RESPECT TO FGM THICKNESS RATIO AND VOLUME FRACTION INDEX

n	r_f			
	0	0.4	0.6	1
0.2	0.3494	0.3492	0.3494	0.3510
0.5	0.3494	0.3490	0.3488	0.3422
1	0.3494	0.3488	0.3480	0.3315
2	0.3494	0.3484	0.3470	0.3150
5	0.3494	0.3476	0.3450	0.2786

Through-the-thickness distribution of the stress ratio $\sigma*$ for ZrO_2/Ti-6Al-4V FGM composite plates is described in Fig. 5, when the FGM thickness ratio is 0.4 for (a) and 1 for (b). In Fig. 5(a), when n is 0.2, small stress concentration is observed at the FGM-ceramic interface ($\bar{z}$ =0.7). However, when n is 5, the stress concentration is considerable at the metal-FGM layer interface ($\bar{z}$ =0.3). In Fig. 5(b), it is shown that the stress concentration is relaxed, while the tensile stress increases greatly in the region $\bar{z} \leq 0.5$, especially when n is 5. Furthermore, compressive stress increases in the region $\bar{z} \geq 0.5$, when n is 0.2. In overall view of the responses, the smoothest stress distribution is observed in the case of n =0.2.

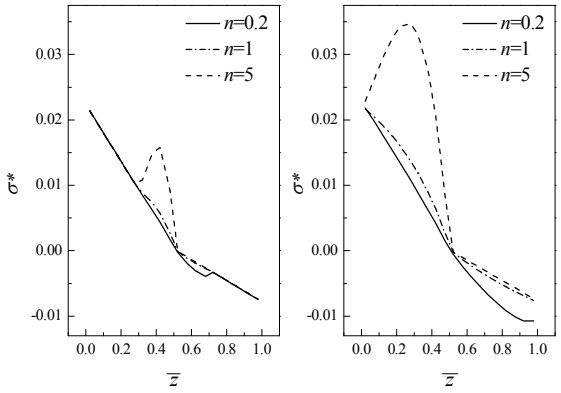

(a) r_f =0.4 (b) r_f =1

Fig. 5 Through-the-thickness distribution of the stress ratio $\sigma*$ with variation of volume fraction index

As a result, for the smallest n and for the fully FGM plates, the absolute value of stress ratio $|\sigma*|$ has the smallest value and the stress distribution shows the smoothest response.

Fig. 6 presents the distribution of maximum stress ratio for Si_3N_4/SUS304, Al_2O_3/Ni and ZrO_2/Ti-6Al-4V FGM plates with variation of volume fraction index. It is observed that Si_3N_4/SUS304 FGM plate has the largest value of $|\sigma*|_{\max}$ generally, while ZrO_2/Ti-6Al-4V FGM plate has the smallest value. This shows that ZrO_2/Ti-6Al-4V FGM plate has the smallest stress ratio in three cases.

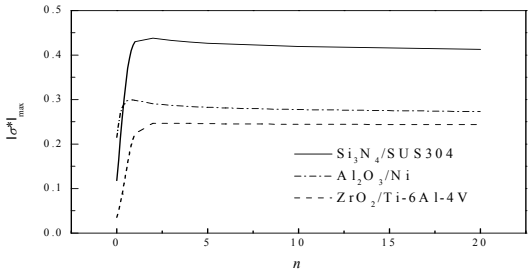

Fig. 6 Distribution of maximum stress ratio $|\sigma*|_{\max}$ for FGM plates with variation of volume fraction index r_f equal to1.

V. CONCLUSION

The stress analysis under mechanical load of FGM composite plates are investigated using 3-D finite element method. Si_3N_4/SUS304, Al_2O_3/Ni and ZrO_2/Ti-6Al-4V are used for material constituents. The 18-node solid element is selected for more accurate modeling of material properties in the thickness direction. Material properties are assumed to be temperature

dependent, and in FGM layer with varying continuously in the thickness direction. To obtain the volume fraction in FGM, simple power law distribution is applied. The effective material properties, temperature and position dependent, is obtained using linear rule of mixtures.

For stress analysis, the tensile and compressive stress ratios of the structure under sinusoidal load are investigated. The effects of the FGM thickness ratio, volume fraction distribution, geometric parameter and mechanical load on the tensile and compressive stress ratios are investigated. When the volume fraction index is increased, the compressive stress ratio decrease. The minimum compressive stress ratio are observed for the fully FGM plate with largest volume fraction index. The tensile stress ratio has the smallest value for the fully FGM plate with smallest volume fraction index. The maximum tensile stress ratio is larger than the maximum compressive stress ratio. Thus, the tensile stress ratio is the most important value for evaluation of maximum stress ratio. The stress ratio distribution shows the smoothest response for the fully FGM plate with smallest volume fraction index. Furthermore, it is observed that ZrO_2/Ti-6Al-4V FGM plate has the smallest stress ratio in three material cases.

REFERENCES

[1] J. N. Reddy and C. D. Chin, "Thermomechanical analysis of functionally graded cylinders and plates," *J. Thermal Stresses.*, vol. 21, 1998, pp. 593-626.

[2] K. S. Na and J. H. Kim, "Three-dimensional thermal buckling analysis of functionally graded materials," *Compos. Part B, Engng.*, vol. 35, no. 5, 2004, pp. 429-437.

[3] M. M. Najafizadeh and M. R. Eslami, "First-order-theory-based thermoelastic stability of functionally graded material circular plates, " *AIAA J.*, vol. 40, no. 7, 2002, pp. 1444-1450.

[4] T. Nakamura, T. Wang and S. Sampath, "Determination of properties of graded materials by inverse analysis and instrumented indentation," *Acta. Mater.*, vol. 48, 2000, pp. 4293-4306.

[5] J. Yang and H. S. Shen, "Nonlinear bending analysis of shear deformable functionally graded plates subjected to thermo-mechanical loads under various boundary conditions," *Compos. Part B, Engng.*, vol. 34, 2003, pp. 103-115.

[6] L. S. Ma and T. J. Wang, "Nonlinear bending and post-buckling of a functionally graded circular plate under mechanical and thermal loadings," *Int. J. Solids Struct.*, vol. 40, 2003, pp. 3311-3330.

[7] S. S. Vel and R. C. Batra, "Three-dimensional analysis of transient thermal stresses in functionally graded plates," *Int. J. Solids Struct.*, vol. 40, 2003, pp. 7181-7196.

[8] L. F. Qian, R. C. Batra and L. .M. Chen, "Static and dynamic deformations of thick functionally graded elastic plates by using higher-order shear and normal deformable plate theory and meshless local Petrov-Galerkin method, " *Compos. Part B, Engng.*, vol. 35, 2004, pp. 685-697.

[9] Z. H. Jin and R. C. Batra, "R-curve and strength behavior of a functionally graded material," *Mater. Sci. Engng.*, vol. 242, 1998, pp. 70-76.

[10] K. Tanaka, H. Watanabe, Y. Sugano and V. F. Poterasu, "A multicriterial material tailoring of a hollow cylinder in functionally gradient materials: Scheme to global reduction of thermoelastic stresses," *Comput. Methods Appl. Mech. Engng.*, vol. 135, 1996, pp. 369-380.

[11] C. Li, Z. Zou and Z. Duan, "Stress intensity factors for functionally graded solid cylinders," *Engng. Fracture Mech.*, vol. 63, 1999, pp. 735-749.

[12] Y. Ootao, Y. Tanigawa and O. Ishimaru, "Optimization of material composition of functionally graded plate for thermal stress relaxation using a genetic algorithm," *J. Thermal Stresses.*, vol. 23, 2000, pp. 257-271.

[13] J. R. Cho and J. H. Choi, "A yield-criteria tailoring of the volume fraction in metal-ceramic functionally graded material," *Eur. J. Mech. A/Solids.*, vol. 23, 2004, pp. 271-281.